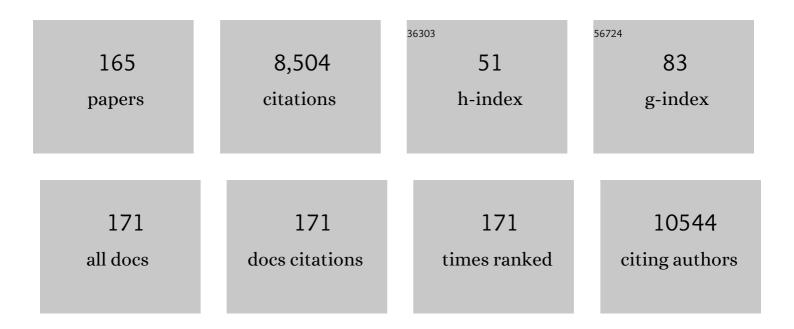


List of Publications by Year in descending order

Source: https://exaly.com/author-pdf/5527137/publications.pdf Version: 2024-02-01



H-V VII

#	Article	IF	CITATIONS
1	Versatile sensing devices for self-driven designated therapy based on robust breathable composite films. Nano Research, 2022, 15, 1027-1038.	10.4	33
2	Flexible, anti-damage, and non-contact sensing electronic skin implanted with MWCNT to block public pathogens contact infection. Nano Research, 2022, 15, 2616-2625.	10.4	19
3	Novel ultrasonic-coating technology to design robust, highly sensitive and wearable textile sensors with conductive nanocelluloses. Chemical Engineering Journal, 2022, 428, 131289.	12.7	40
4	A comprehensive investigation on cellulose nanocrystals with different crystal structures from cotton via an efficient route. Carbohydrate Polymers, 2022, 276, 118766.	10.2	48
5	Lightweight Nanofibrous Crosslinked Composite Aerogels with Controllable Shapes and Superelasticity for Pressure Sensors. Macromolecular Materials and Engineering, 2022, 307, .	3.6	5
6	Simultaneously Enhance the Heat Storage Capacity and Shape Stability of Poly(hexadecyl acrylate) by Immobilizing It to Cellulose Nanocrystal via In Situ Free Radical Polymerization. ACS Applied Polymer Materials, 2022, 4, 899-907.	4.4	0
7	Chain-ring covalently interconnected cellulose nanofiber/MWCNT aerogel for supercapacitors and sensors. Nanoscale, 2022, 14, 5163-5173.	5.6	8
8	Electroconductive cellulose nanocrystals — Synthesis, properties and applications: A review. Carbohydrate Polymers, 2022, 289, 119419.	10.2	19
9	Interface Growth of PANI-ZnO Nanohybrids on a Self-Formed Grapefruit Peel Aerogel to Construct a Quick Self-Restored Gas Sensor. ACS Sustainable Chemistry and Engineering, 2022, 10, 6573-6583.	6.7	13
10	Novel strategy to interpret the degradation behaviors and mechanisms of bio- and non-degradable plastics. Journal of Cleaner Production, 2022, 355, 131757.	9.3	20
11	Nanocellulose-based functional materials for advanced energy and sensor applications. Nano Research, 2022, 15, 7432-7452.	10.4	24
12	Freezing-induced interfacial growth of polypyrrole layers on hierarchical carbon aerogels for robust ultrasensitive pressure sensors. Industrial Crops and Products, 2022, 186, 115215.	5.2	8
13	"Soft-rigid―synergistic reinforcement of PHBV composites with functionalized cellulose nanocrystals and amorphous recycled polycarbonate. Composites Part B: Engineering, 2021, 206, 108542.	12.0	34
14	Magnetic cellulose nanocrystals hybrids reinforced phase change fiber composites with highly thermal energy storage efficiencies. Carbohydrate Polymers, 2021, 254, 117481.	10.2	18
15	Degradation mechanism of green biopolyester nanocomposites with various cellulose nanocrystal based nanohybrids. Cellulose, 2021, 28, 7735-7748.	4.9	22
16	Versatile nanocellulose-based nanohybrids: A promising-new class for active packaging applications. International Journal of Biological Macromolecules, 2021, 182, 1915-1930.	7.5	23
17	Construction of Nanocellulose Aerogels with Mechanical Flexibility and pH-Responsive Properties via a Cross-Linker Structure Design Strategy. ACS Sustainable Chemistry and Engineering, 2021, 9, 9951-9960.	6.7	9
18	Confined Chemical Transitions for Direct Extraction of Conductive Cellulose Nanofibers with Graphitized Carbon Shell at Low Temperature and Pressure. Journal of the American Chemical Society, 2021, 143, 11620-11630.	13.7	43

#	Article	IF	CITATIONS
19	Multifunctional Biosensors Made with Self-Healable Silk Fibroin Imitating Skin. ACS Applied Materials & Interfaces, 2021, 13, 33371-33382.	8.0	27
20	Selective adsorption and separation of organic dyes using functionalized cellulose nanocrystals. Chemical Engineering Journal, 2021, 417, 129237.	12.7	116
21	Continuous Meter-Scale Wet-Spinning of Cornlike Composite Fibers for Eco-Friendly Multifunctional Electronics. ACS Applied Materials & Interfaces, 2021, 13, 40953-40963.	8.0	25
22	Highly sensitive self-healable strain biosensors based on robust transparent conductive nanocellulose nanocomposites: Relationship between percolated network and sensing mechanism. Biosensors and Bioelectronics, 2021, 191, 113467.	10.1	25
23	An environmentally friendly and economical strategy to cyclically produce cellulose nanocrystals with high thermal stability and high yield. Green Chemistry, 2021, 23, 4866-4872.	9.0	21
24	Cellulose nanofiber derived carbon aerogel with 3D multiscale pore architecture for high-performance supercapacitors. Nanoscale, 2021, 13, 17837-17845.	5.6	31
25	The Fabrication of Cassava Silk Fibroin-Based Composite Film with Graphene Oxide and Chitosan Quaternary Ammonium Salt as a Biodegradable Membrane Material. Autex Research Journal, 2021, 21, 459-466.	1.1	2
26	Sensitive, Stretchable, and Sustainable Conductive Cellulose Nanocrystal Composite for Human Motion Detection. ACS Sustainable Chemistry and Engineering, 2021, 9, 17351-17361.	6.7	16
27	Smart nonwoven fabric with reversibly dual-stimuli responsive wettability for intelligent oil-water separation and pollutants removal. Journal of Hazardous Materials, 2020, 383, 121123.	12.4	65
28	A freestanding nitrogen-doped carbon nanofiber/MoS2 nanoflowers with expanded interlayer for long cycle-life lithium-ion batteries. Journal of Alloys and Compounds, 2020, 818, 152835.	5.5	34
29	Tailoring Commercial Cellulose Membranes into Janus Conductive Electronic Skin via Diffusion-Controlled Polymerization. ACS Sustainable Chemistry and Engineering, 2020, 8, 17458-17465.	6.7	12
30	Flexible ZnO/PANI/nonwoven nanocomposite based high-sensitive NH3 gas sensor via vapor phase polymerization method. Materials Science for Energy Technologies, 2020, 3, 862-867.	1.8	5
31	Ultrasensitive and robust self-healing composite films with reinforcement of multi-branched cellulose nanocrystals. Composites Science and Technology, 2020, 198, 108300.	7.8	26
32	Electrospun Polyethylene Glycol/Polyvinyl Alcohol Composite Nanofibrous Membranes as Shape-Stabilized Solid–Solid Phase Change Materials. Advanced Fiber Materials, 2020, 2, 167-177.	16.1	27
33	Bifunctional Reinforcement of Green Biopolymer Packaging Nanocomposites with Natural Cellulose Nanocrystal–Rosin Hybrids. ACS Applied Bio Materials, 2020, 3, 1944-1954.	4.6	41
34	Supermagnetic cellulose nanocrystal hybrids reinforced PHBV nanocomposites with high sensitivity to intelligently detect water vapor. Industrial Crops and Products, 2020, 154, 112704.	5.2	13
35	High molecular weight of poly(acrylonitrile-co-3-aminocarbonyl-3-butenoic acid methyl ester) used as carbon fiber precursor: preparation and stabilization. Journal of Thermal Analysis and Calorimetry, 2020, 140, 2687-2699.	3.6	1
36	Novel design of Fe-Cu alloy coated cellulose nanocrystals with strong antibacterial ability and efficient Pb2+ removal. Carbohydrate Polymers, 2020, 234, 115889.	10.2	46

#	Article	IF	CITATIONS
37	Shape-Stabilized Cellulose Nanocrystal-Based Phase-Change Materials for Energy Storage. ACS Applied Nano Materials, 2020, 3, 1741-1748.	5.0	35
38	Double stimuli-responsive cellulose nanocrystals reinforced electrospun PHBV composites membrane for intelligent drug release. International Journal of Biological Macromolecules, 2020, 155, 330-339.	7.5	44
39	Fabricating robust soft-hard network of self-healable polyvinyl alcohol composite films with functionalized cellulose nanocrystals. Composites Science and Technology, 2020, 194, 108165.	7.8	43
40	Green acid-free hydrolysis of wasted pomelo peel to produce carboxylated cellulose nanofibers with super absorption/flocculation ability for environmental remediation materials. Chemical Engineering Journal, 2020, 395, 125070.	12.7	97
41	Fabrication of a novel temperature sensitive phase change system based on ZnO@PNIPAM core-satellites and 1-tetradecanol as gatekeeper. Materials Science for Energy Technologies, 2020, 3, 482-486.	1.8	1
42	Robust natural biomaterial based flexible artificial skin sensor with high transparency and multiple signals capture. Chemical Engineering Journal, 2020, 394, 124855.	12.7	40
43	Constructing stimuli-free self-healing, robust and ultrasensitive biocompatible hydrogel sensors with conductive cellulose nanocrystals. Chemical Engineering Journal, 2020, 398, 125547.	12.7	148
44	Highly Efficient and Superfast Cellulose Dissolution by Green Chloride Salts and Its Dissolution Mechanism. ACS Sustainable Chemistry and Engineering, 2020, 8, 18446-18454.	6.7	51
45	Natural Biodegradable Poly(3-hydroxybutyrate- <i>co</i> -3-hydroxyvalerate) Nanocomposites with Multifunctional Cellulose Nanocrystals/Graphene Oxide Hybrids for High-Performance Food Packaging. Journal of Agricultural and Food Chemistry, 2019, 67, 10954-10967.	5.2	85
46	Comprehensive Insight into Degradation Mechanism of Green Biopolyester Nanocomposites Using Functionalized Cellulose Nanocrystals. ACS Sustainable Chemistry and Engineering, 2019, 7, 15537-15547.	6.7	35
47	Facile and Green Synthesis of Carboxylated Cellulose Nanocrystals as Efficient Adsorbents in Wastewater Treatments. ACS Sustainable Chemistry and Engineering, 2019, 7, 18067-18075.	6.7	65
48	Self-Healable Conductive Nanocellulose Nanocomposites for Biocompatible Electronic Skin Sensor Systems. ACS Applied Materials & Interfaces, 2019, 11, 44642-44651.	8.0	84
49	Enhancing long-term biodegradability and UV-shielding performances of transparent polylactic acid nanocomposite films by adding cellulose nanocrystal-zinc oxide hybrids. International Journal of Biological Macromolecules, 2019, 141, 893-905.	7.5	55
50	Teleost Type 2 Interleukin-1 Receptor (IL-1R2) from the Spotted Halibut (Verasper variegatus): 3D Structure and a Role in Immune Response. Molecular Biology, 2019, 53, 256-266.	1.3	2
51	Thermo and light-responsive phase change nanofibers with high energy storage efficiency for energy storage and thermally regulated on–off drug release devices. Chemical Engineering Journal, 2019, 375, 121979.	12.7	54
52	Supramolecular Self-Assembly of 3D Conductive Cellulose Nanofiber Aerogels for Flexible Supercapacitors and Ultrasensitive Sensors. ACS Applied Materials & Interfaces, 2019, 11, 24435-24446.	8.0	120
53	Simple Synthesis of Flower-like Manganese Dioxide Nanostructures on Cellulose Nanocrystals for High-Performance Supercapacitors and Wearable Electrodes. ACS Sustainable Chemistry and Engineering, 2019, 7, 11823-11831.	6.7	35
54	A sustainable biomemristive memory device based on natural collagen. Materials Today Chemistry, 2019, 13, 18-24	3.5	25

#	Article	IF	CITATIONS
55	Multibranch Strategy To Decorate Carboxyl Groups on Cellulose Nanocrystals To Prepare Adsorbent/Flocculants and Pickering Emulsions. ACS Sustainable Chemistry and Engineering, 2019, 7, 6969-6980.	6.7	69
56	Green one-step synthesis of ZnO/cellulose nanocrystal hybrids with modulated morphologies and superfast absorption of cationic dyes. International Journal of Biological Macromolecules, 2019, 132, 51-62.	7.5	78
57	Simple Process To Produce High-Yield Cellulose Nanocrystals Using Recyclable Citric/Hydrochloric Acids. ACS Sustainable Chemistry and Engineering, 2019, 7, 4912-4923.	6.7	96
58	High molecular weight poly(acrylonitrile-co-3-aminocarbonyl-3-butenoic acid methyl ester) prepared by mixed solvent polymerization I. effect of monomer feed ratios on polymerization and stabilization. Journal of Polymer Research, 2019, 26, 1.	2.4	3
59	Designing Highly Luminescent Cellulose Nanocrystals with Modulated Morphology for Multifunctional Bioimaging Materials. ACS Applied Materials & Interfaces, 2019, 11, 48192-48201.	8.0	39
60	Interfacial compatible poly(ethylene glycol) chains modified cellulose nanosphere as bifunctional reinforcements in green polylatic acid for food packagings. Journal of the Taiwan Institute of Chemical Engineers, 2019, 95, 583-593.	5.3	28
61	Chemical cross-linked polyvinyl alcohol/cellulose nanocrystal composite films with high structural stability by spraying Fenton reagent as initiator. International Journal of Biological Macromolecules, 2018, 113, 171-178.	7.5	44
62	Flocculation Performance of Hyperbranched Polyethylenimine-Grafted Cellulose in Wastewater Treatment. ACS Sustainable Chemistry and Engineering, 2018, 6, 1592-1601.	6.7	47
63	Green synthesis of sheet-like cellulose nanocrystal–zinc oxide nanohybrids with multifunctional performance through one-step hydrothermal method. Cellulose, 2018, 25, 6433-6446.	4.9	34
64	High Aspect Ratio Carboxylated Cellulose Nanofibers Cross-linked to Robust Aerogels for Superabsorption–Flocculants: Paving Way from Nanoscale to Macroscale. ACS Applied Materials & Interfaces, 2018, 10, 20755-20766.	8.0	131
65	Green acid-free one-step hydrothermal ammonium persulfate oxidation of viscose fiber wastes to obtain carboxylated spherical cellulose nanocrystals for oil/water Pickering emulsion. Cellulose, 2018, 25, 5139-5155.	4.9	49
66	Novel fabrication of modulated carpenterworm-like zinc oxide/polyacrylonitrile composite nanofibers for photocatalytic degradation of methylene blue dye. Journal of the Taiwan Institute of Chemical Engineers, 2018, 91, 548-555.	5.3	7
67	Sheet-like Cellulose Nanocrystal-ZnO Nanohybrids as Multifunctional Reinforcing Agents in Biopolyester Composite Nanofibers with Ultrahigh UV-Shielding and Antibacterial Performances. ACS Applied Bio Materials, 2018, 1, 714-727.	4.6	79
68	A novel chemical reduction method to fabricate tunable selenium nanosphere and nanobelt based on cellulose nanocrystals. Materials Letters, 2018, 230, 44-47.	2.6	2
69	Electrospun poly(3-hydroxybutyrate-co-3-hydroxy-valerate)/cellulose reinforced nanofibrous membranes with ZnO nanocrystals for antibacterial wound dressings. Cellulose, 2017, 24, 2925-2938.	4.9	81
70	Achieving Long-Term Sustained Drug Delivery for Electrospun Biopolyester Nanofibrous Membranes by Introducing Cellulose Nanocrystals. ACS Biomaterials Science and Engineering, 2017, 3, 1666-1676.	5.2	50
71	Effect of silver contents in cellulose nanocrystal/silver nanohybrids on PHBV crystallization and property improvements. Carbohydrate Polymers, 2017, 173, 7-16.	10.2	47
72	In vitro degradation and possible hydrolytic mechanism of PHBV nanocomposites by incorporating cellulose nanocrystal-ZnO nanohybrids. Carbohydrate Polymers, 2017, 176, 38-49.	10.2	58

#	Article	IF	CITATIONS
73	Cellulose nanocrystals/polyethylene glycol as bifunctional reinforcing/compatibilizing agents in poly(lactic acid) nanofibers for controlling long-term in vitro drug release. Cellulose, 2017, 24, 4461-4477.	4.9	43
74	From Cellulose Nanospheres, Nanorods to Nanofibers: Various Aspect Ratio Induced Nucleation/Reinforcing Effects on Polylactic Acid for Robust-Barrier Food Packaging. ACS Applied Materials & Interfaces, 2017, 9, 43920-43938.	8.0	170
75	Superfast Adsorption–Disinfection Cryogels Decorated with Cellulose Nanocrystal/Zinc Oxide Nanorod Clusters for Water-Purifying Microdevices. ACS Sustainable Chemistry and Engineering, 2017, 5, 6776-6785.	6.7	45
76	Use of electrospinning to directly fabricate three-dimensional nanofiber stacks of cellulose acetate under high relative humidity condition. Cellulose, 2017, 24, 219-229.	4.9	31
77	Facile fabrication of controllable zinc oxide nanorod clusters on polyacrylonitrile nanofibers via repeatedly alternating immersion method. Journal of Nanoparticle Research, 2016, 18, 1.	1.9	17
78	New Approach for Single-Step Extraction of Carboxylated Cellulose Nanocrystals for Their Use As Adsorbents and Flocculants. ACS Sustainable Chemistry and Engineering, 2016, 4, 2632-2643.	6.7	222
79	Temporal responses of microorganisms and native organic carbon mineralization to 13C-glucose addition in a sandy loam soil with long-term fertilization. European Journal of Soil Biology, 2016, 74, 16-22.	3.2	13
80	Reinforcing properties of bacterial polyester with different cellulose nanocrystals via modulating hydrogen bonds. Composites Science and Technology, 2016, 136, 53-60.	7.8	49
81	A high molecular weight acrylonitrile copolymer prepared by mixed solvents polymerization: II. effect of DMSO/water ratios on polymerization and stabilization. Journal of Polymer Research, 2016, 23, 1.	2.4	7
82	Remifentanil tolerance and hyperalgesia: shortâ€ŧerm gain, longâ€ŧerm pain?. Anaesthesia, 2016, 71, 1347-1362.	3.8	167
83	Polylactic acid nanocomposite films with spherical nanocelluloses as efficient nucleation agents: effects on crystallization, mechanical and thermal properties. RSC Advances, 2016, 6, 46008-46018.	3.6	52
84	Single-step extraction of functionalized cellulose nanocrystal and polyvinyl chloride from industrial wallpaper wastes. Industrial Crops and Products, 2016, 89, 66-77.	5.2	23
85	Comparison of international normalized ratio audit parameters in patients enrolled in GARFIELDâ€AF and treated with vitamin K antagonists. British Journal of Haematology, 2016, 174, 610-623.	2.5	13
86	Fabrication of multifunctional cellulose nanocrystals/poly(lactic acid) nanocomposites with silver nanoparticles by spraying method. Carbohydrate Polymers, 2016, 140, 209-219.	10.2	64
87	Flower-like zinc oxide nanorod clusters grown on spherical cellulose nanocrystals via simple chemical precipitation method. Cellulose, 2016, 23, 1871-1884.	4.9	48
88	A universal route for the simultaneous extraction and functionalization of cellulose nanocrystals from industrial and agricultural celluloses. Journal of Nanoparticle Research, 2016, 18, 1.	1.9	22
89	Spherical and rod-like dialdehyde cellulose nanocrystals by sodium periodate oxidation: Optimization with double response surface model and templates for silver nanoparticles. EXPRESS Polymer Letters, 2016, 10, 965-976.	2.1	21
90	Karyotype analysis and ribosomal gene localization of spotted knifejaw Oplegnathus punctatus. Genetics and Molecular Research, 2016, 15, .	0.2	5

#	Article	IF	CITATIONS
91	One-step extraction and functionalization of cellulose nanospheres from lyocell fibers with cellulose II crystal structure. Cellulose, 2015, 22, 3773-3788.	4.9	59
92	Mechanical Properties and Corrosion Resistance of Vulcanized Silicone Rubber after Exposure to Artificial Urine. Journal of Macromolecular Science - Physics, 2015, 54, 962-974.	1.0	11
93	Nitrous oxide emission and nitrogen use efficiency in response to nitrophosphate, N-(n-butyl) thiophosphoric triamide and dicyandiamide of a wheat cultivated soil under sub-humid monsoon conditions. Biogeosciences, 2015, 12, 803-815.	3.3	49
94	Analysis of the expression of HMGB-1, CXCL16, miRNA-30a, and TGF-Î ² 1 in primary nephritic syndrome patients and its significance. Genetics and Molecular Research, 2015, 14, 9841-9848.	0.2	3
95	Goal orientation and employee creativity: The mediating role of creative role identity. Journal of Management and Organization, 2015, 21, 82-97.	3.0	26
96	Silylation of cellulose nanocrystals and their reinforcement of commercial silicone rubber. Journal of Nanoparticle Research, 2015, 17, 1.	1.9	35
97	Importance of heterotrophic nitrification and dissimilatory nitrate reduction to ammonium in a cropland soil: Evidences from a 15N tracing study to literature synthesis. Soil Biology and Biochemistry, 2015, 91, 65-75.	8.8	135
98	Linking organic carbon accumulation to microbial community dynamics in a sandy loam soil: result of 20Âyears compost and inorganic fertilizers repeated application experiment. Biology and Fertility of Soils, 2015, 51, 137-150.	4.3	93
99	Survival analysis of surgically treated renal cell carcinoma: a single Chinese medical center experience from 2002 to 2012. International Urology and Nephrology, 2015, 47, 1327-1333.	1.4	3
100	The dynamics of glucose-derived 13C incorporation into aggregates of a sandy loam soil following two-decade compost or inorganic fertilizer amendments. Soil and Tillage Research, 2015, 148, 14-19.	5.6	19
101	A facile one-pot route for preparing cellulose nanocrystal/zinc oxide nanohybrids with high antibacterial and photocatalytic activity. Cellulose, 2015, 22, 261-273.	4.9	126
102	Sorafenib Neoadjuvant Therapy in the Treatment of High Risk Renal Cell Carcinoma. PLoS ONE, 2015, 10, e0115896.	2.5	30
103	Influence of 20–Year Organic and Inorganic Fertilization on Organic Carbon Accumulation and Microbial Community Structure of Aggregates in an Intensively Cultivated Sandy Loam Soil. PLoS ONE, 2014, 9, e92733.	2.5	57
104	Nitrous oxide emissions from cultivated black soil: A case study in Northeast China and global estimates using empirical model. Global Biogeochemical Cycles, 2014, 28, 1311-1326.	4.9	71
105	Endovascular treatment for secondary aortoduodenal fistula. Surgical Practice, 2014, 18, 98-101.	0.2	1
106	One-pot green fabrication and antibacterial activity of thermally stable corn-like CNC/Ag nanocomposites. Journal of Nanoparticle Research, 2014, 16, 1.	1.9	45
107	Green Nanocomposites Based on Functionalized Cellulose Nanocrystals: A Study on the Relationship between Interfacial Interaction and Property Enhancement. ACS Sustainable Chemistry and Engineering, 2014, 2, 875-886.	6.7	87
108	Biomimicking the structure of silk fibers via cellulose nanocrystal as β-sheet crystallite. RSC Advances, 2014, 4, 14304-14313.	3.6	48

#	Article	IF	CITATIONS
109	Induction of Myogenic Differentiation of Human Mesenchymal Stem Cells Cultured on Notch Agonist (Jagged-1) Modified Biodegradable Scaffold Surface. ACS Applied Materials & Interfaces, 2014, 6, 1652-1661.	8.0	24
110	Fully biodegradable food packaging materials based on functionalized cellulose nanocrystals/poly(3-hydroxybutyrate-co-3-hydroxyvalerate) nanocomposites. RSC Advances, 2014, 4, 59792-59802.	3.6	109
111	Investigating the Spatial Distribution of Integrin β ₁ in Patterned Human Mesenchymal Stem Cells Using Super-Resolution Imaging. ACS Applied Materials & Interfaces, 2014, 6, 15686-15696.	8.0	10
112	Reinforcement of biodegradable poly(3-hydroxybutyrate-co-3-hydroxyvalerate) with cellulose nanocrystal/silver nanohybrids as bifunctional nanofillers. Journal of Materials Chemistry B, 2014, 2, 8479-8489.	5.8	103
113	Reinforcement of transparent poly(3-hydroxybutyrate-co-3-hydroxyvalerate) by incorporation of functionalized carbon nanotubes as a novel bionanocomposite for food packaging. Composites Science and Technology, 2014, 94, 96-104.	7.8	103
114	Surface grafting of cellulose nanocrystals with poly(3-hydroxybutyrate-co-3-hydroxyvalerate). Carbohydrate Polymers, 2014, 101, 471-478.	10.2	62
115	Novel approach to extract thermally stable cellulose nanospheres with high yield. Materials Letters, 2014, 131, 12-15.	2.6	32
116	Cellulose nanocrystals as organic nanofillers for transparent polycarbonate films. Journal of Nanoparticle Research, 2013, 15, 1.	1.9	41
117	Allosteric Activation of Functionally Asymmetric RAF Kinase Dimers. Cell, 2013, 154, 1036-1046.	28.9	236
118	Size influences the cytotoxicity of poly (lactic-co-glycolic acid) (PLGA) and titanium dioxide (TiO2) nanoparticles. Archives of Toxicology, 2013, 87, 1075-1086.	4.2	121
119	Size of TiO2 nanoparticles influences their phototoxicity: an in vitro investigation. Archives of Toxicology, 2013, 87, 99-109.	4.2	87
120	Comparison of the reinforcing effects for cellulose nanocrystals obtained by sulfuric and hydrochloric acid hydrolysis on the mechanical and thermal properties of bacterial polyester. Composites Science and Technology, 2013, 87, 22-28.	7.8	113
121	A Generic Micropatterning Platform to Direct Human Mesenchymal Stem Cells from Different Origins Towards Myogenic Differentiation. Macromolecular Bioscience, 2013, 13, 799-807.	4.1	17
122	Facile extraction of thermally stable cellulose nanocrystals with a high yield of 93% through hydrochloric acid hydrolysis under hydrothermal conditions. Journal of Materials Chemistry A, 2013, 1, 3938.	10.3	391
123	Functional Morphometric Analysis in Cellular Behaviors: Shape and Size Matter. Advanced Healthcare Materials, 2013, 2, 1188-1197.	7.6	39
124	A Bioâ€inspired Platform to Modulate Myogenic Differentiation of Human Mesenchymal Stem Cells Through Focal Adhesion Regulation. Advanced Healthcare Materials, 2013, 2, 442-449.	7.6	40
125	Listeners' Attitudes Toward Children With Voice Problems. Journal of Speech, Language, and Hearing Research, 2013, 56, 1409-1415.	1.6	39
126	Rac1 Activation in Podocytes Induces Rapid Foot Process Effacement and Proteinuria. Molecular and Cellular Biology, 2013, 33, 4755-4764.	2.3	107

#	Article	IF	CITATIONS
127	Insights into the Role of Focal Adhesion Modulation in Myogenic Differentiation of Human Mesenchymal Stem Cells. Stem Cells and Development, 2013, 22, 136-147.	2.1	42
128	Comparison of covalent and noncovalent interactions of carbon nanotubes on the crystallization behavior and thermal properties of poly(3â€hydroxybutyrateâ€ <i>co</i> â€3â€hydroxyvalerate). Journal of Applied Polymer Science, 2013, 130, 4299-4307.	2.6	17
129	Research on Mechanism of Capturing of Customers' Requirements in Process of Concept Design. , 2013, , 419-426.		0
130	Enhanced Heat Conduction in Cellulose Nanocrystals Grafting Polyethylene Glycol as Solid-Solid Phase Change Materials. Advanced Materials Research, 2012, 557-559, 563-566.	0.3	1
131	Tissue specific expression of Pax3/7 and MyoD in adult duck tissues. Journal of Applied Animal Research, 2012, 40, 284-288.	1.2	2
132	Simultaneous improvement of mechanical properties and thermal stability of bacterial polyester by cellulose nanocrystals. Carbohydrate Polymers, 2012, 89, 971-978.	10.2	119
133	Cyclic tensile loading regulates human mesenchymal stem cell differentiation into neuron-like phenotype. Journal of Tissue Engineering and Regenerative Medicine, 2012, 6, s68-s79.	2.7	28
134	Injection of duck recombinant follistatin fusion protein into duck muscle tissues stimulates satellite cell proliferation and muscle fiber hypertrophy. Applied Microbiology and Biotechnology, 2012, 94, 1255-1263.	3.6	12
135	A novel and simple microcontact printing technique for tacky, soft substrates and/or complex surfaces in soft tissue engineering. Acta Biomaterialia, 2012, 8, 1267-1272.	8.3	42
136	Crystallization behavior and hydrophobic properties of biodegradable ethyl cellulose-g-poly(3-hydroxybutyrate-co-3-hydroxyvalerate): The influence of the side-chain length and grafting density. Carbohydrate Polymers, 2012, 87, 2447-2454.	10.2	38
137	In ovo feeding of IGFâ€1 to ducks influences neonatal skeletal muscle hypertrophy and muscle mass growth upon satellite cell activation. Journal of Cellular Physiology, 2012, 227, 1465-1475.	4.1	23
138	Cellulose nanocrystals as green fillers to improve crystallization and hydrophilic property of poly(3-hydroxybutyrate-co-3-hydroxyvalerate). Progress in Natural Science: Materials International, 2011, 21, 478-484.	4.4	93
139	Characterization of in vitro cultured myoblasts isolated from duck (Anas platyrhynchos) embryo. Cytotechnology, 2011, 63, 399-406.	1.6	13
140	Bioâ€inspired Micropatterned Platform to Steer Stem Cell Differentiation. Small, 2011, 7, 1416-1421.	10.0	52
141	Mutation that blocks ATP binding creates a pseudokinase stabilizing the scaffolding function of kinase suppressor of Ras, CRAF and BRAF. Proceedings of the National Academy of Sciences of the United States of America, 2011, 108, 6067-6072.	7.1	116
142	In ovo administration of rhIGF-1 to duck eggs affects the expression of myogenic transcription factors and muscle mass during late embryo development. Journal of Applied Physiology, 2011, 111, 1789-1797.	2.5	23
143	Enhancement in optical transmission of ZnO: Al film by c-orientation arrayed growth. International Journal of Materials Research, 2011, 102, 556-559.	0.3	2
144	Arhgap24 inactivates Rac1 in mouse podocytes, and a mutant form is associated with familial focal segmental glomerulosclerosis. Journal of Clinical Investigation, 2011, 121, 4127-4137.	8.2	234

#	Article	IF	CITATIONS
145	Cell-Matrix Interaction Study during Human Mesenchymal Stem Cells Differentiation. IFMBE Proceedings, 2011, , 51-51.	0.3	0
146	Micropatterned matrix directs differentiation of human mesenchymal stem cells towards myocardial lineage. Experimental Cell Research, 2010, 316, 1159-1168.	2.6	148
147	Porous polycaprolactone scaffold for cardiac tissue engineering fabricated by selective laser sintering. Acta Biomaterialia, 2010, 6, 2028-2034.	8.3	310
148	Cellular behavior of human mesenchymal stem cells cultured on single-walled carbon nanotube film. Carbon, 2010, 48, 1095-1104.	10.3	94
149	A preliminary framework for geometric basis computing pattern. , 2010, , .		0
150	Multiscale Topological Guidance for Cell Alignment via Direct Laser Writing on Biodegradable Polymer. Tissue Engineering - Part C: Methods, 2010, 16, 1011-1021.	2.1	64
151	Mechanical behavior of human mesenchymal stem cells during adipogenic and osteogenic differentiation. Biochemical and Biophysical Research Communications, 2010, 393, 150-155.	2.1	98
152	Thickness sensing of hMSCs on collagen gel directs stem cell fate. Biochemical and Biophysical Research Communications, 2010, 401, 287-292.	2.1	74
153	An event-related potential study of the concreteness effect between Chinese nouns and verbs. Brain Research, 2009, 1253, 149-160.	2.2	34
154	Adjuvant Therapy for the Reduction of Postoperative Intra-abdominal Adhesion Formation. Asian Journal of Surgery, 2009, 32, 180-186.	0.4	35
155	A Hybrid Non-strict Implicit Constraints Solving Algorithm. , 2009, , .		0
156	Clinical Features, Polysomnography and Outcome in Patients with Hypnic Headache. Cephalalgia, 2008, 28, 209-215.	3.9	52
157	An Improved Mass-Spring Model to Simulate Draping Cloth. , 2008, , .		2
158	Photodetection of basal cell carcinoma using methyl 5-aminolaevulinate-induced protoporphyrin IX based on fluorescence image analysis. Clinical and Experimental Dermatology, 2007, 32, 423-429.	1.3	23
159	The psychological burden experienced by Hong Kong midlife women during the SARS epidemic. Stress and Health, 2005, 21, 177-184.	2.6	63
160	Accelerated apoptosis in the Timp-3–deficient mammary gland. Journal of Clinical Investigation, 2001, 108, 831-841.	8.2	142
161	Chlorhexidine for Irrigation of Vas: a Clinical Trial and the Study of Viability of Nonâ€Motile Sperms in Postâ€Vasectomy Patients with Trypan Blue Uptake. British Journal of Urology, 1976, 48, 371-375.	0.1	13
162	Optimization of Plastic Injection Molding Process Parameters for Thin-Wall Plastics Injection Molding. Advanced Materials Research, 0, 69-70, 525-529.	0.3	3

#	ARTICLE	IF	CITATIONS
163	A Cloth Simulation Method for Cloth/ Machinery Coupled System Unified Modeling. Applied Mechanics and Materials, 0, 37-38, 1-4.	0.2	Ο
164	Effects of Microcrystalline Cellulose on the Thermal Properties of Poly(3-hydroxybutyrate- <i>co</i> -3-hydroxyvalerate). Advanced Materials Research, 0, 284-286, 1778-1781.	0.3	7
165	Effect of Cellulose Nanocrystal on Crystallization Behavior of Poly(3–hydroxybutyrate–co–3–hydroxyvalerate). Advanced Materials Research, 0, 430-432, 20-23.	0.3	4